Journal of Materials and Environmental Science
ISSN : 2028-2508
e-ISSN : 2737-890X
CODEN : JMESCN

J. Mater. Environ. Sci., 2024, Volume 15, Issue 6, Page 893-915

http://www.jmaterenvironsci.com

Kinetics, equilibrium, and thermodynamics studies of Methylene Blue Dye adsorption onto modified activated carbon produced from groundnut shells

Umar Isah Abubakar[1,2], Mustapha Abdullahi[1,3]*, and Hamza Abdulhamid[2]**

[1]*Product and Process Development (PPD) Research Group, Department of Chemical Engineering, Faculty of Engineering, Ahmadu Bello University, Zaria, Nigeria*
[2]*Office of the Head, Department of Chemical Engineering, Ahmadu Bello University Zaria, Nigeria.*
[3]*National Environmental Standards and Regulations Enforcement Agency, Kaduna Office, Federal Ministry of Environment, Abuja, Nigeria*

**Corresponding author, Email address: mustaphaabdullahi4@gmail.com*
***Corresponding author, Email address: iaumar@abu.edu.ng*

Received *29 May 2024,*
Revised *23 June 2024,*
Accepted *30 June 2024*

Keywords:
- ✓ *Modified groundnut shell activated carbon;*
- ✓ *Adsorption;*
- ✓ *Kinetics;*
- ✓ *Equilibrium;*
- ✓ *Thermodynamics;*
- ✓ *Methylene Blue dye*

Citation*: Isah U. A., Abdullahi M., and Abdul-Hamid H. (2024) Kinetics, equilibrium, and thermodynamics studies of Methylene Blue dye adsorption onto modified groundnut shell activated carbon, J. Mater. Environ. Sci., 15(6), 893-915*

Abstract: In this work, modified groundnut shell activated carbons (MGSAC) were produced from agricultural by-products for the kinetics, equilibrium, and thermodynamics studies of Methylene Blue (MB) dye adsorption from aqueous solution. MGSAC was characterized using the Scanning electron microscopy (SEM), Fourier transforms infrared spectroscopy (FT-IR), UV/visible spectrophotometer, and pH point zero of surface charge (pHpzc). The experiments for the kinetics, isotherms, thermodynamics adsorption studies were conducted in batches in order to examine the influence of initial dye concentration (25–100 mg/L), contact time (5–80 min), temperatures (30–45°C), and pH (3–11) on the adsorption of MB dye The observed experimental data was found to be best described by pseudo 2nd order kinetic model. The activation energy (E_A) was determined as 6.35 kJ/mol. It was noted that the observed specific adsorption rate constant, k_{obs} decreased by 2.9 and 53 folds with increase in activation energy, E_A from 44.987 to 58.084 and to 70.213kJ/mol when the initial dye concentration was changed from 25 mg/L to 50 mg/L, and 100 mg/L, respectively. Langmuir equilibrium adsorption isotherm model best fitted the observed equilibrium adsorption experimental data with R^2 values of 0.995, 0.9873, 0.9929 and 0.993 and the least RSS at operating temperature of 303 K, 308 K, 313 K, and 318 K, respectively. The maximum monolayer adsorption capacity was found to be 65.49mg/g. Thermodynamic analysis reveals that the adsorption process was endothermic and spontaneous, the changes in entropy (ΔS) were found to be between 189 and 260 J/mol while the enthalpy (ΔH) were found to be 45.092 and 70.5350 kJ/mol within the range of initial concentration (25-100 mg/L), respectively. MGSAC was shown to be a promising adsorbent for the adsorption of MB dye from aqueous solutions with high sticking probability (S*<<1).

1. Introduction

The outcomes of the kinetics, equilibrium, and thermodynamics studies of adsorption processes resulted in having vast vital information about the pertinent data require for the successful accomplishment of the end product(s) and process(es) of the goals for process development. These studies are crucial parts of process research and development (R&D). They play an essential role in the

profitable design, operation, improvement, and commercialization of new and existing adsorbent products for the adsorption processes (Isah *et al.*, 2022, Isah *et al.*, 2015, Isah *et al.*, 2023). Adsorption rate constants, order of the adsorption process are the relevant kinetic parameters profoundly required in characterizing the rate of adsorption and the adsorber design. The other parameters that disclose and dictate the feasibility and nature of the process include the changes in the standard enthalpy, entropy, and Gibbs free energy in addition to the useful and valuable parameters of the equilibrium adsorption isotherms. These pertinent data are needed in the design and development of any type of adsorber at different scales such as bench, pilot, and commercial sizes. Several studies have been reported on the adsorption kinetics, isotherms, and thermodynamics studies of different forms of dyes onto various kinds of adsorbent/sorbents produced through turning wastes of agricultural products into wealth (Isah *et al.*, 2022, Islam *et al.*, 2015, Hameed *el al.*, 2007, Salman and Alsaad (2012), Rasool and Lee (2015), Isah *et al.*, 2015, Isah *et al.*, 2023, Wang *et al.*, 2016, Al Othman *et al.*, 2013, Ebrahimi *et al.*, 013, Ahmad *et al.*, 2014, Aljeboree *et al.*, 2015, Danish *et al.*, 2018, Das and Mishra (2017), Zubair *et al.*, 2017, Torğut and Demirelli (2018), Sarabadan *et al.*, 2019, Al-Asadi *et al.*, 2023).

There is a growing concern about the environmental protection over the years from the global perspective (Foo and Hameed, 2010). This resulted due to the rapid population expansion, urbanisation with rapidly changing technologies, large throughputs of commodity and industrial products with their processes generating wastes and pollutants into the water bodies across the globe that are highly threatening to the environment and public health due to improper management (Isah *et al.*, 2023, Qiu *al.*, 2015). The intermediate products of the dye manufacturing industry are extensively used in various industries ranging from textile, pulp and paper, ink, cosmetics, plastics, tannery, leather, to food and pharmaceuticals (Isah *et al.*, 2023). It has been reported that more than 10,000 different kinds of synthetic dyes and pigments are commercially available. About 10-15% of the dyes are lost in the effluents in the course of dyeing process (Najim and Yassin, 2009, Isah *et al.*, 2022, Isah *et al.*, 2015, Foo and Hameed, 2010). In addition, some of the recent studies have shown that the presence of coloured dyes in the wastewater effluents may result chemical and biological changes, consume dissolved oxygen from the stream, and prevent reoxygenation (Foo and Hameed, 2010, Isah *et al.*, 2015). Generally, dyes are known to be toxic, mutagenic, and carcinogenic, can cause cyanosis, dermatitis, quadriplegia, tissue necrosis, allergy, eye or skin infections, irritation, and aesthetic pollution if they are spew into water bodies, and are not degradable by conventional aerobic treatment due to their recalcitrance (Yaqub *et al.*, 2014, Qiu *et al.*, 2015, Yaseen and Scholz, 2018).

Many techniques have been extensively used for the conventional treatments and removal of dyes from wastewater and are available. These include coagulation–flocculation, and sedimentation technologies; reverse osmosis, nanofiltration and dialysis membrane methods, aerobic and anaerobic degradation microbiological methods; and chemical oxidation technologies using Fenton's reagent with hydrogen peroxide, photo-catalysis with UV radiation and ozonation; ion exchange resins using electrochemical methods, and adsorption technologies using adsorbents such as activated carbon, inorganic adsorbents such as silica or clays (Foo and Hameed, 2010). However, adsorption technology utilizing activated carbon (AC) as an adsorbent has been found one of the most promising and proven technologies, cost effective physical technique for the adsorption of pollutants from wastewater due to its low cost, and other good features for environmentally friendliness (Abdullahi 2009; Salman *et al.*, 2012; Sekirifa *et al.*, 2012; Oladipo *et al.*, 2013; Mohammed *et al.*, 2014; Sivashankar *et al.*, 2014; Das and Mishara, 2017; Zoha *et al.*, 2020; Kankou *et al.* 2021).

Activated carbons (ACs) can be produced chemically or physically or combination of both chemical and physical techniques from any potential carbonaceous material. For chemical process, the activation

of carbonaceous material is done with metallic chlorides such as zinc chloride, mild acids like phosphoric acids, bases such as potassium hydroxide or sodium hydroxide prior to carbonization. Similarly, physical activation together with carbonization can be carried out under high temperature operations with steam or inert gases such as nitrogen gas. On the other hand, simultaneous chemical and physical activation can be combined with carbonization and conducted under high temperature operations with steam or inert gases such as nitrogen gas (Abdullahi, 2009, Muhammad, 2010, Alslaibi *et al.*, 2013, Islam *et al.*, 2015, Danish and Ahmad, 2018, Alahabadi *et al.*, 2020, Li *et al.*, 2015, Wu *et al*., 2019, Kumari et al., 2020). von Ostreyko (1901) set the basis for the first commercial process development of activated carbon (Dąbrowski, 2001). Subsequently, several reports have been reported for the utilization of carbonaceous materials such as coal, wood, lignite, corncobs, and coconut shells for the commercial production of activated carbons (Li *et al.*, 2002, Vernersson *et al.*, 2002, Rafatullah *et al.*, 2010, Teshome, 2015, Wang *et al.*, 2020). 3,7-bis(dimethylamino) phenothiazine chloride tetra methylthionine chloride known as methylene blue (MB), it is one of the synthetic dyes that largely applied as colorant for papers, in wool, silk, and cotton (Oladoye *et al.*, 2022). Several works focused to find suitable technique for remove this dye causing environmental pollution and harmful to human health (Aaddouz *et al.*, 2023).

Therefore, the main objective of this study was to explore the prospects for improving our results of research findings from previous work on groundnut shell activated carbon (GSAC) products from groundnut shells agricultural byproducts activated chemically with phosphoric acid (H_3PO_4) through the use of ethylenediaminetetraacetic acid disodium salt (Na_2EDTA) as a modifier targeted for the kinetics, equilibrium, and thermodynamic studies of Methylene Blue (MB) dye adsorption in line with our bigger picture ongoing project for the process development of commercial size adsorber.

2. Material and Methods

2.1 Materials

The materials, equipment and other facilities used in the research investigations include the following groundnut shells agricultural byproducts obtained from Samaru Zaria, distilled water obtained from Chemical Engineering, A.B.U. Zaria, phosphoric acid with purity of 85% w/w procured from BDH Chemicals Ltd, England, disodium ethylenediamine tetraacetate (Na_2EDTA) with 99% w/w purity purchased from Kermel, France, Methylene Blue (99% w/w) procured from Sigma Aldrich, Germany, sodium chloride (NaCl) with 99% w/w purity, sodium hydroxide (NaOH) with 99.5% w/w purity, hydrochloric acid (HCl) with 36% w/w purity, a Mufler tubular furnace (Gallenkamp), pH meter (pHep®), oven (Gallenkamp hot box oven), a Scanning Electron Microscope (SEM), a Fourier Transform Infrared (FTIR) spectroscope, and a UV-VIS Spectrophotometer (SHARCHTECH 752N).

2.2 Production of modified groundnut shell activated carbon

The preliminary processes involved cleaning, drying, and particle size reduction of the groundnut shells with water to eliminate contaminants, oven drying at 105°C for 24 hours, and then grinding with a crusher to have the ground particles of groundnut shells, respectively. The production of the modified groundnut shell activated carbons combined both chemical and physical methods. 50g sample of groundnut shells were thoroughly mixed with 50 cm^3 of 35 mmol disodium ethylenediamine tetraacetate (Na_2EDTA) for modification, and then impregnated with 50 cm^3 of phosphoric acid (H_3PO_4) solution at different concentrations of 50, 60, and 70 % w/w for chemical activation over 24 hours. The mixtures were then placed in a Gallenkamp Mufler tube furnace for simultaneous physical

activation and carbonization under inert environment by heating at the rate of 10^0C/min until the desired temperatures of 350, 400, and 450°C were reached and maintained for various activation times of 10, 20, and 30 minutes under a constant nitrogen gas flow of 100 mL/min. The products were then cooled at room temperature. The product yield of modified activated carbon produced from groundnut shells (MGSAC) was calculated as the ratio of the weight of dried activated carbon to the initial weight of the raw groundnut shell (RGS) agricultural byproduct. This process parameter can be calculated in percentage as shown in equation (1). The products of modified groundnuts shell activated carbons were washed repeatedly with distilled water until the pH falls between 6.7 and 7.0. Finally, the products were dried in an oven at 110 °C for 24 hours, grounded, stored in an airtight container, and subsequently used for characterizations, and adsorption experimental studies.

$$Yield, \mathrm{Y} = \frac{W_2}{W_1} \times 100 \qquad (1)$$

Where W_2 and W_1 are the weights for the final modified activated carbon (g) produced and the raw material (groundnut) shell (g), respectively.

2.3 Characterization of modified groundnut shell activated carbon

The modified groundnut shell activated carbon (MGSAC) were characterized using various analytical techniques such as the determination of pH point of zero surface charge (pHpzc) using a modified pH drift technique reported by Bello and Ahmad (2012) and Jawad *et al*., (2020), analysis of Fourier Transforms Infrared Spectroscopy (FT-IR), and Scanning Electron Microscopy (SEM) for viewing the surface morphology of the products).

2.4 Synthesis of model adsorbate

Methylene Blue (MB) dye is a cationic basic, hazardous substance with excellent adsorption properties. It has a wavelength and molecular weights of 664 nm and 319.85 g/mol, respectively. It was chosen as the model adsorbate in this research studies due to its wide applications. The molecular structures of MB dye with their is shown in Figure 1. Stock solution of Methylene Blue (MB) dye was made by dissolving 1.0 g of dye in 1 L of distilled water.

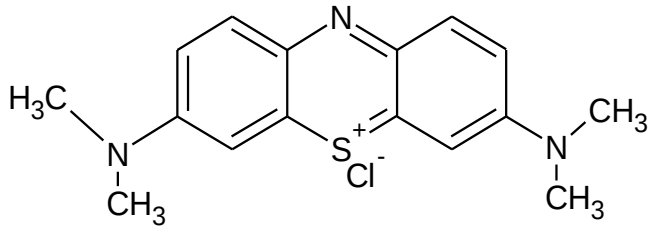

Figure 1. Molecular structures of Methylene Blue (MB) dye.

All working solutions of MB dye concentrations of 25, 50, 75, and 100 mg/L were prepared from the stock solution by dilution with distilled water. The pH of the solution was adjusted and maintained by adding 0.1 M NaOH or HCl.

2.5 Studies for the adsorption kinetics, equilibrium, and thermodynamics

The adsorption experiments for the studies of kinetics, equilibrium, and thermodynamics were carried out in batch mode. A 50 mL of 25 mg/L of the standard working solutions of the MB dye solution was mixed with 0.1 g of the MGSAC adsorbent in a 250 mL conical flask for 60 min under ambient temperature of 28±1ºC. Then, the mixture was agitated thoroughly at the temperature of 30°C, 35°C, 40°C, and 45°C with constant speed of 200 rpm of a magnetic stirrer for pH from (3–11), initial dye concentration from (25–100 mg/L) and contact time from (5–80 min) in a hot plate. After the process attaining equilibrium, a fine tip syringe was used to take samples from the mixture at regular intervals, which were then filtered through Whatman No. 42 filter paper. The absorbance of each filtered sample was observed, measured, and recorded at the maximum wavelength λ_{max} of 664 nm of the MB dye solutions using UV/Visible-Spectrophotometer (SHARCHTECH 752N UV-VIS Spectrophotometer) at the beginning and at the end of each experiment. The adsorption efficiency of MB dye onto MGSAC was determined using equation 2. On the other hand, the quantity of adsorbate adsorbed at equilibrium, q_e (mg/g) and the quantity of adsorbate, q_t (mg/g) at time *t,* of MB dye were determined using equations 3 and 4, respectively. The adsorption experiments for both studies of kinetics and equilibrium were similar. Nevertheless, the only difference was in the case of kinetics studies where observation, noting, and recording of the specified process time is of paramount importance.

$$E_A = \frac{C_0 - C_e}{C_0} \times 100 \quad (2)$$

$$q_e = \frac{C_0 - C_e}{M} \times V \quad (3)$$

$$q_t = \frac{C_0 - C_t}{M} \times V \quad (4)$$

Where M is the mass of the adsorbent used (g), C_0, C_e, C_t (mg/L) are the liquid phase concentrations of adsorbate MB dye at initial, equilibrium, at any time *t* (min), respectively, E_A is the MB dye adsorption efficiency in (%) and *V* is the volume of the solution (mL).

2.5.1 Studies for the adsorption kinetics

In this investigation, the kinetic data were generated at the specified contact time intervals from (5-80 min) and with initial concentrations from (25-100 mg/L) at constant MGSAC dosage of 0.1g/L in 250 mL conical flasks, and agitated at 200 rpm, and keeping other parameters explained in section 2.5 unchanged. The kinetics of MB dye adsorption onto MGSAC was described through the kinetic models for pseudo-first-order, pseudo-second order and intra-particle diffusion.

Kinetic model expression for the pseudo first-order adsorption

The pseudo first-order adsorption rate law for the MB dye onto MGSAC can be expressed according to Lagergren, (1898) as shown in equation 5.

$$\frac{dq_t}{dt} = k_1(q_e - q_t) \quad (5)$$

where k_1 (min^{-1}) is the observed specific rate constant for the pseudo first-order adsorption kinetic model expression. Using the boundary conditions: $q_t = 0$ at $t = 0$ and $q_t = q_t$ at $t = t$ for integrating equation 5, and rearranging into a linear form gives equation 6:

$$log(q_e - q_t) = logq_e - \frac{k_1}{2.303}t \quad (6)$$

It is observed that q_e and k_1 can be estimated from the intercept and slope of the plots of $log(q_e - q_t)$ versus t for different kinetic data at different conditions as shown in equation 6.

Kinetic model expression for the pseudo second order adsorption

Likewise, the rate law for the pseudo second-order adsorption of MB dye onto the MGSAC can be expressed based on the relation reported by Ho and McKay (1999) as shown in equation 7.

$$\frac{dq_t}{dt} = k_2(q_e - q_t)^2 \quad (7)$$

where k_2 (min g mg^{-1}) is the observed specific rate constant for the pseudo second-order adsorption kinetic model. Using the boundary conditions: $q_t = 0$ at $t = 0$ and $q_t = q_t$ at $t = t$ for integrating equation 7, and rearranging into a linear form results equation 8.

$$\frac{t}{q_t} = \frac{1}{k_2 q^2{}_e} + \frac{t}{q_e} \quad (8)$$

The initial rate for the adsorption of MB dye can be considered from equation 8 when t approaches 0, to be as shown in equation 8.

$$r_{A0} = k_2 q^2{}_e \quad (9)$$

Thus, the initial rate for the adsorption of MB dye, r_{A0}(mg $L^{-1}min^{-1}$), q_e and qe can be estimated experimentally from the slope and intercept of the plots of t/q_t versus t for different kinetic data at different conditions as shown in equation 8 and 9.

Diffusion model expression for the intra-particle adsorption

The chances for intra-particle diffusion step to be the rate limiting for the adsorption of MB dye onto the MGSAC was examined using the expression reported by Weber and Morris (1963) as shown in equation 10.

$$q_t = k_{id}t^{1/2} + C_i \quad (10)$$

where C_i is the resistance to the mass transfer across the film, and k_{id} is the adsorption rate constant for intra-particle diffusion. If intra-particle diffusion controls the process (i.e. the rate-limiting step), then plots of q_t versus the square root of time ($t^{1/2}$) would give a straight line. The values of k_{id} and C_i can be found from the slope and intercept of the equation 10 plots.

The influence of temperature on the adsorption

The influence of temperature on the adsorption of the MB dye onto the MGSAC was examined by varying the temperature regimes of the adsorption which in turn affects the activation energy of the

process and might have dominant effects on the specific adsorption rate constant. The expression reported by Arrhenius (1889) as shown in equation 11, modified Arrhenius equation, and the concept of sticking probability in relation to surface coverage employed by many researchers (Aljeboree *et al.*, 2015, Najim and Yassin, 2009; Elg *et al.*, 1997) were used in estimating the activation energy of the adsorption process, and investigating whether the mechanism of adsorption is governed by physisorption or chemisorption.

$$k(T) = Ae^{\frac{-E_A}{RT}} \tag{11}$$

Taking the logarithms both sides of equation (11) gives equation (12):

$$lnk(T) = lnA - \frac{E_A}{R}\left(\frac{1}{T}\right) \tag{12}$$

where k is the specific rate constant of adsorption, A is the frequency factor or pre-exponential factor, R is the universal gas constant (8.314 J mol^{-1} K^{-1}), E is the activation energy, (J mol^{-1}), and T is the absolute temperature (K). E_A can be evaluated experimentally from the slope of the plots of $lnk(T)$ against (1/T) for different temperatures as shown in equation 12.

$$S^* = (1 - \theta)e^{\frac{E_A}{RT}} \tag{13}$$

Taking the logarithms both sides of equation (13) and rearranging gives equation (14):

$$ln(1 - \theta) = lnS^* + \frac{E_A}{RT} \tag{14}$$

The sticking probability S*, is a function of the ratio of adsorbate to adsorbent system under investigation, its value lies in the range $0<S^*<1$ for preferable process and is dependent on the temperature of the system. Where the parameter S^* represents the potential of an adsorbate to persist on the adsorbent. The surface coverage Θ can be determined using the equation 15:

$$\theta = \left(1 - \frac{C_e}{C_o}\right) \quad \text{or} \quad \frac{C_e}{C_0} = (1 - \theta) \tag{15}$$

The values of E_a and S^* can be estimated from the slope and intercept of the plots of $ln(1 - \theta)$ against 1/T, respectively.

2.5.2 Studies for the adsorption equilibrium

In this study, the equilibrium data were generated by selecting the best contact time for the adsorption of MB dye that attained equilibrium from previous adsorption kinetic studies and varying the initial concentrations from (25–100 mg/L) at constant MGSAC dosage of 0.1g/L in 250 mL conical flasks and agitated at 200 rpm and keeping other stated parameters in section 2.5 unchanged. The experimental procedures were repeated by changing the temperatures from (30–45°C). For high diluted solutions, the interactions between the molecules of the dissolved adsorbate and the adsorbent can be neglected, and the process can be described based on the consideration of single-gas adsorption (Dąbrowski, 2001). Hence, the relationship correlating the quantity of the adsorbent (MGSAC) used in adsorbing the amount of adsorbate (MB dye) at equilibrium as a function of concentration at constant temperature was depicted using Langmuir, Freundlich, Temkin, and Dubinin- Radushkevich for the expressions of adsorption isotherm models.

Langmuir model expression for the adsorption isotherms

The adsorption isotherms for Langmuir (1916) have been used extensively to represent the adsorption of adsorbate based on the concepts of monolayer on energetically uniform homogeneous solid surfaces. This is done based on the assumptions that there are no interactions among the adsorbate molecules and have the same attraction for the impinging molecules. The Langmuir isotherm model expression can be written in linear form as shown in equation 16:

$$\frac{C_e}{q_e} = \frac{1}{K_A q_m} + \frac{1}{q_m} C_e \qquad (16)$$

where K_A is the Langmuir constant, which is related to the energy of adsorption (L/mg) and the affinity of the binding sites, and q_m is the maximum adsorption capacity (mg/g). K_A and q_m can be found from the intercept and slope of the plot of C_e/q_e against C_e. Alternatively, equation 16 can be rearranged to give equation 17 as:

$$\frac{1}{q_e} = \frac{1}{q_m} + \frac{1}{K_A q_m C_e} \qquad (17)$$

K_A and q_m can be determined from the slope and intercept of the plot of $1/q_e$ versus $1/C_e$ of equation 17.

Freundlich model expression for the adsorption isotherms

Freundlich (1907) model expression for the adsorption isotherms have been employed in depicting the adsorption processes for the cases of non-ideal adsorption with nonuniform heterogeneous surfaces and occur at sites of different energy levels, as shown in equation 18:

$$q_e = K_f C_e^{\frac{1}{n}} \qquad (18)$$

where K_f and n are the constants of Freundlich isotherms. K_f gives the adsorption capacity, while $1/n$ is the adsorption intensity.

Equation 19 is the linear form of equation 18 for the Freundlich adsorption isotherms.

$$lnq_e = lnK_f + \left(\frac{1}{n}\right) lnC_e \qquad (19)$$

The constants of Freundlich isotherm K_f and n can be estimated from the plot of ln q_e versus ln C_e.

Temkin model expression for the adsorption isotherms

The Temkin model expressions proposed by Temkin (1940) for the adsorption isotherms considers the impact of indirect adsorbate/adsorbate interactions on the adsorption process. Moreover, it assumes that the heat of adsorption of all molecules in the layer reduces linearly as surface coverage increases. However, the isotherms are used only for certain intermediate range of ion concentrations. The linear form of Temkin isotherms can be expressed as shown in equation 20:

$$q_e = \frac{RT}{b_T} InA_T + \left(\frac{RT}{b_T}\right) InC_e \qquad (20)$$

where q_e (mg/g) is the quantity of MB dye adsorbed at equilibrium, and Ce (mg/L) is MB dye concentration at equilibrium. b_T (kJ/mol) and A_T (L/g) are Temkin constants that are relate the heat of

adsorption and maximum binding energy. T is temperature (K), while R (8.314 J/mol.K) is universal gas constant.

Dubinin-Radushkevich model expression for the adsorption isotherms

The Dubinin-Radushkevich (D–R) model for the adsorption isotherms as shown in equation 21 has been utilized to empirically describe the adsorption mechanism with Gaussian energy distribution on heterogeneous surfaces for physical adsorption processes (Dubinin, 1960). D–R model adsorption isotherms has additional capability over other models for accounting temperature dependency. In addition, D–R model is commonly used to distinguish between physical and chemical adsorption. It is based on assumption of multilayer phenomenon involving *Van Der Waal's* forces. The D–R model is only used for intermediate adsorbate concentrations because of its unrealistic asymptotic behavior and limitations in predicting the constants for Henry's laws at low pressure.

$$\mathrm{Inq_e} = \mathrm{Inq_s} - \beta\varepsilon^2 \qquad (21)$$

where ε can be correlated:

$$\varepsilon = \mathrm{RTIn}\left(1 + \frac{1}{\mathrm{C_e}}\right) \qquad (22)$$

where R is the gas constant (8.314 J/mol K) and T is the absolute temperature. A plot of ln q_e against. ε^2 enables the constants q_s and E to be determined.

Mean free energy (*E*) of sorption per molecule of the sorbate when it is transported to the surface of the solid from infinity in the solution as shown in equation 23. Where β represents the constant of the mean free energy equation.

$$\mathrm{E} = \frac{1}{\sqrt{-2\beta}} \qquad (23)$$

2.5.3 Studies for the adsorption thermodynamics

In the thermodynamic studies, some thermodynamic parameters are essential in understanding the nature and feasibility of adsorption process. These parameters include the changes in the standard enthalpy (ΔH°), standard entropy (ΔS°), and standard Gibbs free energy (ΔG°), and hence they are needed to be determined. Changes in Gibbs free energy can be found at constant temperature and from Van't Hoff relation as shown in equations 19 and 20, respectively. The MB dye adsorption on modified groundnut shell activated carbon (MGSAC) was conducted by changing the temperatures from (30–45°C) with varying the initial concentrations from (25–100 mg/L) at constant MGSAC dosage of 0.1g/L in 250 mL conical flasks and agitated at 200 rpm and keeping other parameters described in section 2.5 unchanged.

$$\Delta G^{\circ} = \Delta H^{\circ} - T\Delta S^{\circ} \qquad (24)$$

$$\Delta G^{\circ} = -RTlnK_d \qquad (25)$$

Equating equations 24 and 25 and solving for ΔS° and ΔH° gives:

$$lnK_d = \frac{\Delta S^\circ}{R} - \frac{\Delta H^\circ}{RT} \quad (26)$$

where K_d is the coefficient of distribution which is assumed to be equivalent to q_e/C_e.

3. Results and Discussion

3.1 Production and characterization of modified groundnut shell activated carbon

Modified groundnut shells activated carbon (MGSAC) was produced and the products were characterized using various analytical techniques. Scanning electron microscopy (SEM) was employed for the detailed viewing of microstructure of the activated carbon morphology derived from groundnut shells as shown in Figure 2.

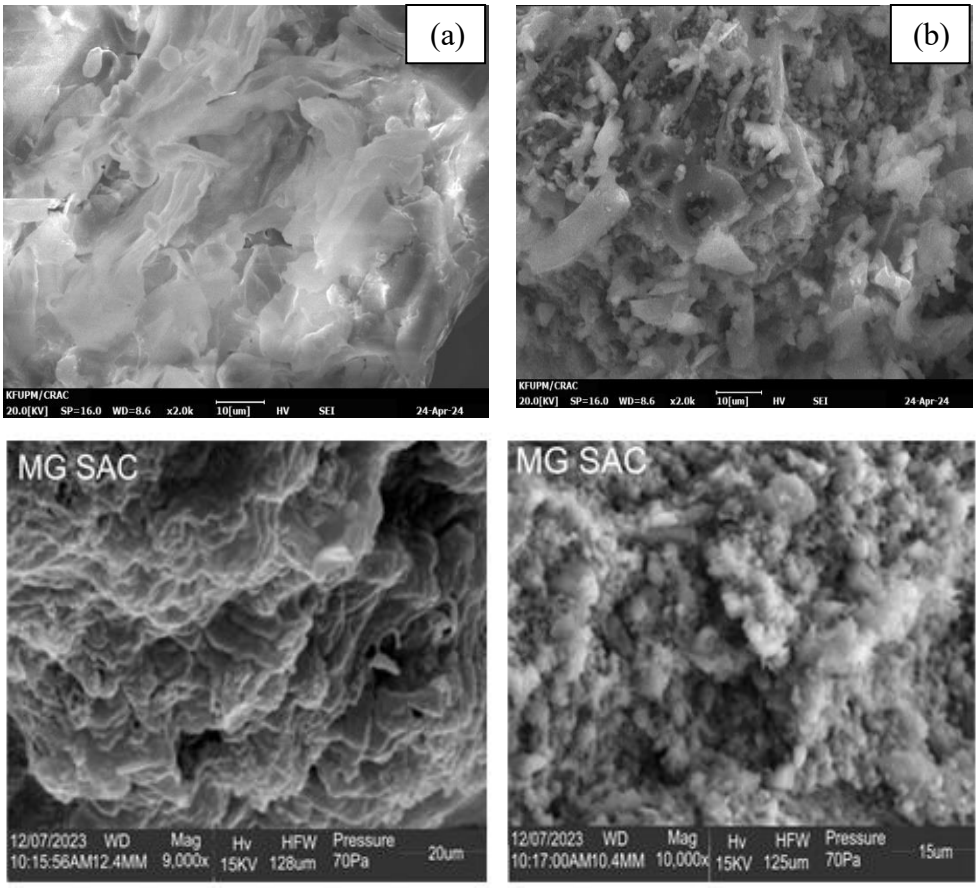

(c) **(d)**

Figure 2. SEM micrograph for (a) Raw Groundnut Shells (RGS) at magnification of X2.0k, and (b, c, and d) Modified Groundnut shell Activated Carbon (MGSAC) produced at magnification of X2.0 k, 9000X and 10,000X simultaneously chemically and physically activated with H_3PO_4 and modified with Na_2EDTA in a Mufler tube furnace.

It can be observed from the SEM micrographs of the RGS and MGSAC. A stiff-like structure can be clearly seen from the RGS while that of MGSACs show fluffy-like structures with multiple pores, demonstrating that high temperature activation in the presence of modifying chemicals promotes the formation of porous structures. Moreover, it can be noted that the holes extended into the interior of the carbonaceous material, an indication that the product has potentiality for excellent dye molecule penetration and adsorption.

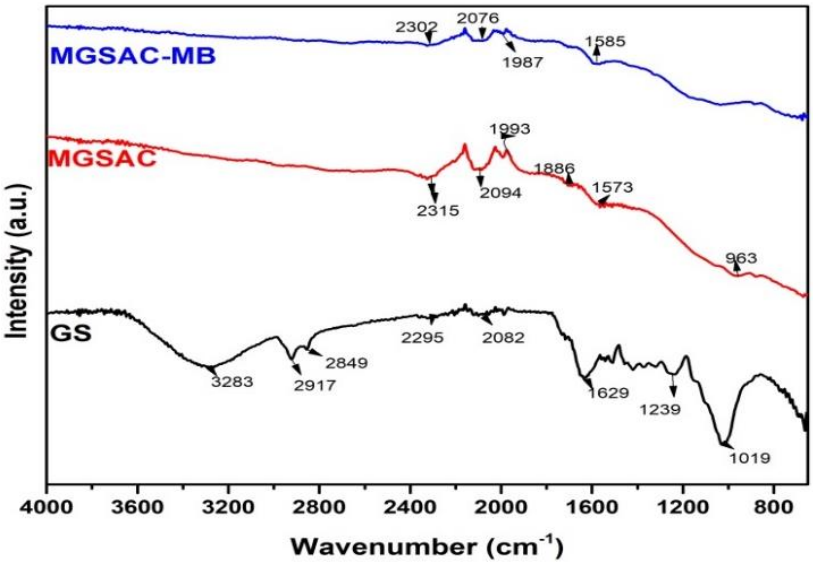

Figure 3. FT-IR analysis for raw groundnut shell, modified groundnut shell activated carbon, and modified groundnut shell activated carbon after methylene blue adsorption.

Figure 3 compares the FT-IR spectra of groundnut shell (GS), modified groundnut shell activated carbon (MGSAC), and modified groundnut shell activated with methylene blue (MGSAC-MB) adsorbed. Different functional groups such as OH and C-H aromatic, C-H aliphatic, C=O and C-O stretching were found in the raw material and products. For the GS, the peaks at 3283 cm^{-1} show -OH group vibrations, whereas the spectrum bands at 2917 and 2849 cm^{-1} suggest aliphatic -CH group vibrations. Peaks at 1629 cm^{-1} correspond to carbonyl -C=O stretching vibrations in carbonyl compounds such as ketones, aldehydes, alkenes, esters, and -C=C of aromatic groups. The peak at 1239 cm^{-1} corresponds to amine-C-N stretching or carboxylic acid-C-O vibration. The peak at 1019 cm^{-1} was attributed to stretching vibrations of -C-O in cellulose and hemicellulose. A few other researchers have observed similar FTIR spectra for biomass (Argun *et al*., 2008).

Groundnut shell modification with the activating agent and carbonization removed the functional groups at 3283 cm^{-1}, 2917 cm^{-1}, and 2849 cm^{-1} attributed to -OH group and aliphatic -CH group stretching vibration. These groups may have been transformed into volatiles, resulting in the creation of additional pores and increased porosity (Saka, 2012).

After modification, the MGSAC revealed additional peaks at 1993 and 1886 cm^{-1}, corresponding to the -C=C=C stretching groups of alkenes (allene group) (Saka, 2012), which were absent in the groundnut shell. The characteristic of C≡C stretch in alkynes ranges from 2295 to 2315 cm^{-1}. The absorption bands at 2295 cm^{-1} on the GS moved to 2351 cm^{-1} after MGSAC modification, and then to 2302 cm^{-1} on methylene blue adsorption (Saka, 2012). Morever, peaks at 1573 cm^{-1} indicated N=C or C=C stretching vibrations in the aromatic ring. These peaks migrated to 1585 cm^{-1} after methylene blue according to several reports. The allene groups of aromatic rings were found at 2082 cm^{-1} on the GS, shifting to 2094 cm^{-1} following modification and 2076 cm^{-1} on MB dye adsorption. After MB dye adsorption, the characteristic peak at 1886 cm^{-1} disappeared and the characteristic peak at 1993 cm^{-1} shifted to 1987 cm^{-1}, indicating the involvement of π–π interactions in the adsorption of methylene blue (Jawad *et al*., 2020).

The pH point of zero surface charge (pHpzc) values were determined by locating the point where the generated curves intersected the pH axis, as illustrated in Figure 4. RGS and MGSAC had pHpzc

values of 6.8 and 4.3, respectively. It can be seen from Figure 4 that the surfaces of MGSAC and RGS are acidic and almost neutral, respectively. The pHpzc is the pH at which the adsorbent's surface charge density is neutral. The surface charge is positive when the pH of the solution is less than pHpzc, and negative when the pH is more than pHpzc. MB dye adsorption is improved at pH levels greater than pHpzc. Farahani *et al*., (2011) reported that an increase in pH above the pzc promotes cationic dye adsorption on adsorbents. Similarly, El-Sayed *et al*., (2014) reported the values of pHpzc of 5.7 for corncob based activated carbon.

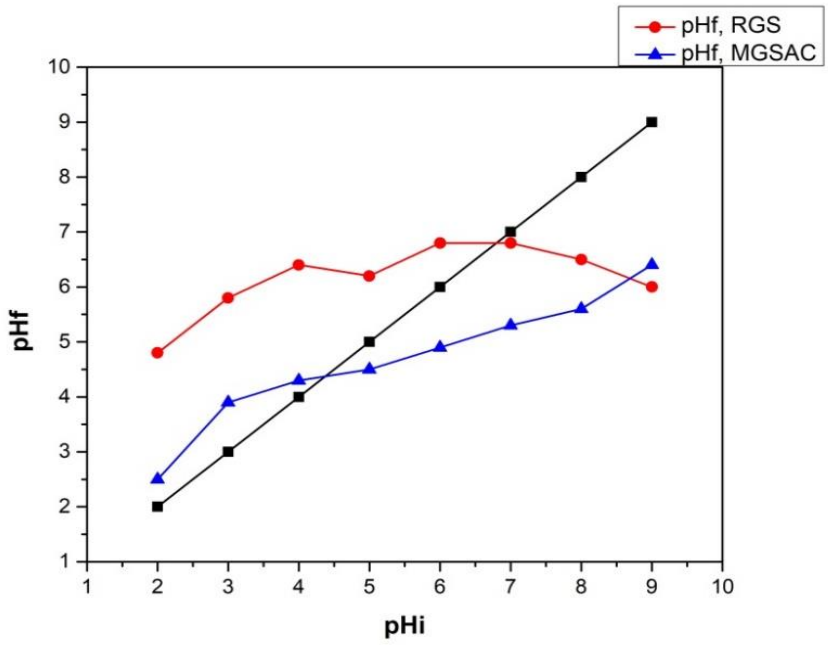

Figure 4. RGS and MGSAC pH point of surface charge (pHpzc)

3.2 Influence of Process Variables for MB dye adsorption of onto MGSAC

3.2.1 Influence of initial dye concentration and contact time on the adsorption of MB dye

The effects of initial dye concentration and contact time for the adsorption of MB dye onto MGSAC are depicted in Figure 5. It can be observed that the amount of MB dye adsorbed by the MGSAC at equilibrium increased rapidly from 12.45 to 49.23 mg/g as the initial dye concentration increased from 25 to 100 mg/L. This impact can be due to the increased driving force of mass transfer of MB dye molecules into active pores within the inner pores of MGSAC at higher initial dye concentrations (Hameed *et al*., 2008). This indicates that the initial MB dye concentration plays a significant role in the adsorption capacity of MB dye onto MGSAC. Similarly, there were several observations reported for the adsorption of MB dye onto the surfaces of various AC materials obtained from different biomass sources. In addition, it can be noted from Figure 5 that the adsorption capacity of MB dye at the outset of all initial concentrations increases very rapidly as the contact time increases. However, it was gradually becoming steady when the process approaches equilibrium and started to be decreasing. This was due to the presence of more unoccupied active surface sites on MGSAC for the uptake of MB dye molecules at early stage of the adsorption process. As the process progresses the contact time increases due to the decrease in the number of active surface sites and saturation of the available surface sites, and consequently slowing down the adsorption process.

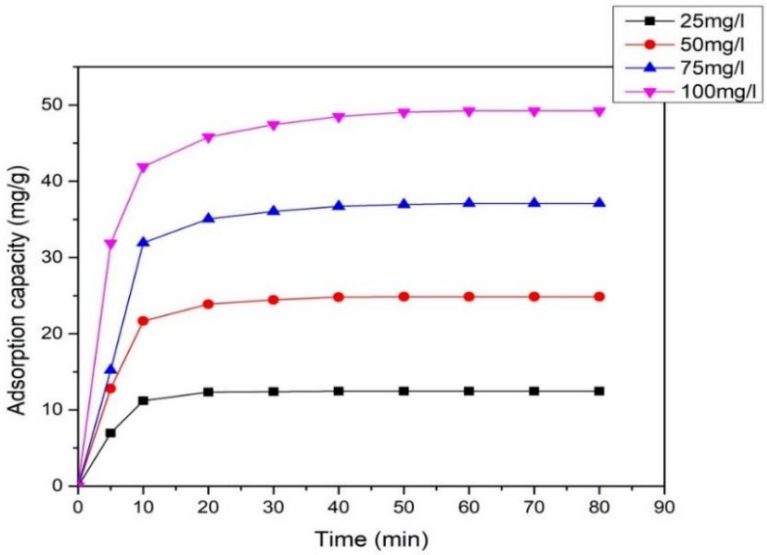

Figure 5. Influence of initial dye concentration and contact time on the adsorption of MB dye.

3.2.2 Influence of temperature and initial dye concentration on the adsorption of MB dye

Figure 6 exhibited the influence of temperature and the initial dye concentration process variables for the adsorption of MB dye onto MGSAC. It can be seen clearly from Figure 6 as the temperature increases with the decrease of initial dye concentrations, the efficiency, and the percentage of MB dye adsorption onto MGSAC increases.

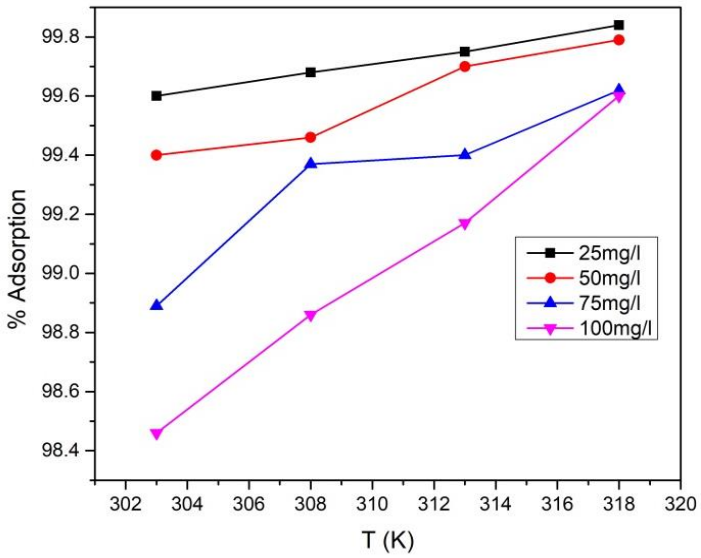

Figure 6. Influence of temperature and initial dye concentration on the adsorption of MB dye.

The rise in temperature increases the rate of diffusion of the solute from the adsorbate to the active surface sites of the MGSAC adsorbent, thereby increasing the overall rate of MB dye adsorption, and hence resulting in high adsorption capacity (Sulaiman *et al*., 2021). On the other hand, at high initial MB dye concentrations, the efficiency, and the percentage of MB dye adsorption onto MGSAC was decreased due to a greater number of adsorbate ions to adsorbent surface-active sites ratio. As a result, the extra high temperature driving force may be required to facilitate MB dye adsorption to a greater extent by increasing the rate of diffusion of solutes from the adsorbate to the surface active sites of MGSAC if an increase in temperature favors the adsorption process, and in turn increases the overall

rate of MB dye adsorption than only the role of the surface characteristics of the MGSAC for favoring the MB dye adsorption.

3.3 Analysis for adsorption kinetics

The results found from the model fittings of MB dye adsorption onto the MGSAC with pseudo first-order, pseudo second-order kinetic model expressions, and intra-particle diffusion using Lageren, (1898); Weber and Morris (1963) under ambient condition are shown in Figures 7, 8 and 9, respectively.

3.3.1 Analysis for the pseudo-first-order kinetics

The kinetic parameters, first-order specific rate constant, k_1, and the adsorption capacity at equilibrium, q_e found from analysis of the pseudo-first order can be seen as shown in Figure 7, and Table 1 for MB dye adsorption onto MGSAC using different initial dye concentration. It can be noted from the Figure 7 that the kinetic model expression of the pseudo-first order did not fit well the observed generated experimental kinetic data. For this reason, it can be seen that the values of calculated adsorption capacity, ($q_{e,\ cal.}$) are not close to the observed values of the experimental adsorption capacity ($q_{e,\ exp.}$) values based on their disparity in the values of correlation coefficients (R^2) and large differences in their values of residual sum of square (RSS). As a result, MB dye adsorption on MGSAC did not fit well with the pseudo-first-order kinetic model. A similar result was observed by Suleiman *et al*., (2021) from generated kinetic data reported in the open literature using cassava stem as the adsorbents for the MB dye adsorption.

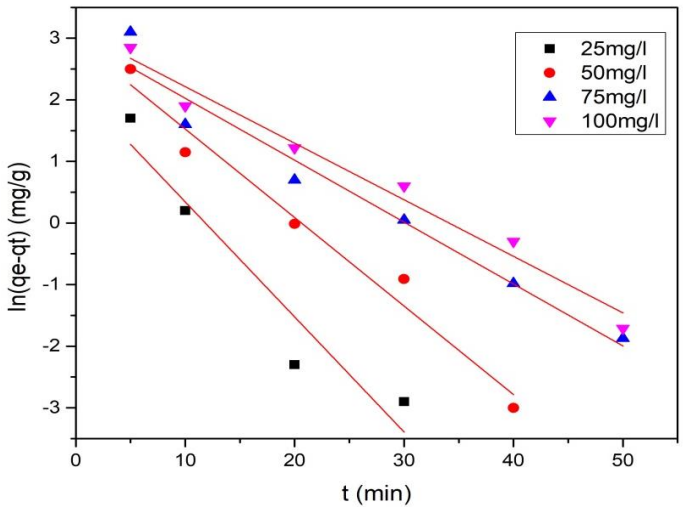

Figure 7. Pseudo-first-order kinetics for MB dye adsorption onto the MGSAC under ambient condition of different initial dye concentration regimes at optimal pH of 7.

3.3.2 Analysis for the pseudo-second-order kinetics

Table 1 displays the values of the pseudo-second-order kinetic parameters with their R^2 and RSS for each of the initial MB dye concentration. It can be observed that the expression for the pseudo-second-order kinetic model best fitted the observed generated kinetic experimental data with the best values of correlation coefficients (R^2) and residual sum of square (RSS) values as shown in Figure 8 and Table 1. Thus, it can be inferred that the pseudo-second-order kinetic model best described the kinetics of MB dye adsorption onto MGSAC.

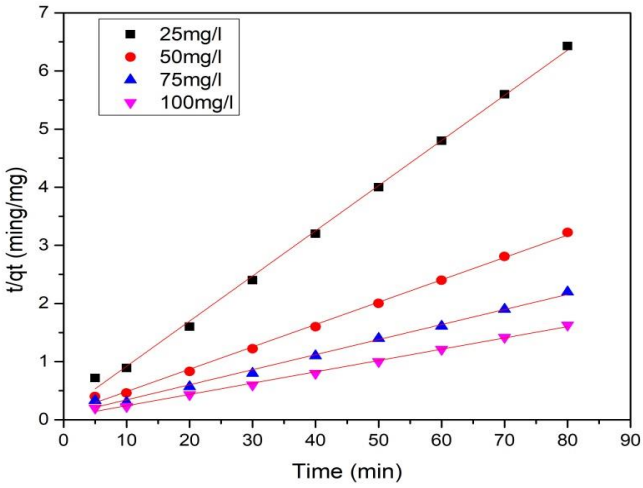

Figure 8. Pseudo-second-order kinetics for MB dye adsorption onto the MGSAC under ambient condition of different initial dye concentration regimes at optimal pH of 7.

In comparison between the closeness of the calculated adsorption capacity values, ($q_{e,\,cal.}$) and that of the experimental adsorption capacity values, ($q_{e,\,exp.}$), the pseudo-second-order kinetic model has the closest values of $q_{e,\,cal}$ to the values of $q_{e,\,exp.}$. than that of the pseudo-first-order kinetic model.

Parameters	25 (mg/L)	50 (mg/L)	75 (mg/L)	100 (mg/L)
1. Pseudo-First order Mode				
$q_{e\ exp.}$ (mg/g)	12.45	24.85	37.09	49.23
k_1 (L/(min)	0.18678	0.14369	0.10052	0.09182
q_e (mg/g)	9.12	19.35	20.70	22.92
R^2	0.8875	0.96506	0.95094	0.97086
RSS	1.04305	0.68749	0.62773	0.30609
2. Pseudo-Second order Model				
$q_{e\ exp.}$ (mg/g)	12.45	24.85	37.09	49.23
k_2 g/(mg/min)	0.0424	0.0147	0.000795	0.000805
q_e (mg/g)	12.87	26.01	38.62	51.44
R^2	0.99798	0.99738	0.99285	0.99674
RSS	0.06009	0.01913	0.00237	0.00609
3. Weber and Morris Intraparticle diffusion model				
$q_{e\ exp.}$ (mg/g)	12.45	24.85	37.09	49.23
k_{id} ($mg.g^{-1}.min^{-0.5}$)	0.56593	1.29648	2.32097	2.11871
C_i (mg/g)	8.30033	15.24991	19.80881	33.14316
R^2	0.45407	0.51901	0.51201	0.69226
RSS	12.63493	52.69021	73.15646	71.3525

Moreover, Islam *et al.* (2015) reported similar trend of results for MB dye adsorption by different forms of adsorbents, such as palm date seed activated carbon. Likewise, the results presented by Fu et al. (2015) for poly dopamine microspheres and that reported by Shi *et al.* (2014) using anaerobic

granular sludge-based biochar. Consequently, the pseudo-second-order kinetic model implies that the adsorption rate is totally controlled by chemisorption via electron sharing or exchange between MB dye adsorbate and MGSAC adsorbent. (Ho and McKay 1999).

3.3.3 Analysis of the model for the Intra-particle diffusion

The chances for the for intra-particle diffusion step to be the rate limiting of for the overall adsorption rate of MB dye adsorption was analyzed using Webber and Morris model.

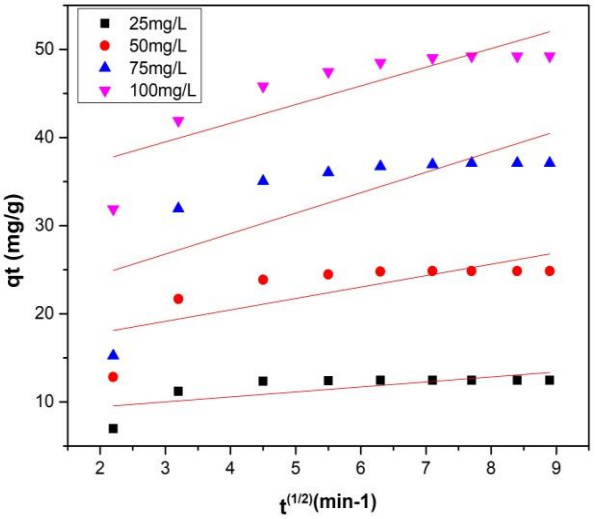

Figure 9. Intra-particle diffusion kinetics for MB dye adsorption onto the MGSAC under ambient condition of different initial dye concentration regimes at optimal pH of 7.

The results of MB dye adsorption onto MGSAC at different initial dye concentration regimes are exhibited in Figure 9 and Table 1. The values of k_{id} were obtained from the slope of the model expression for the intra-particle diffusion and are shown in Table 1. The values of C_i for each of the initial dye concentration are not equal to zero. The result from the linear plots for the adsorption of MB dye onto MGSAC implies that the mechanism of adsorption cannot not be governed as chemisorption and described by Weber and Morris intra-particle diffusion kinetic model. There are some results of similar trends reported for the adsorption of MB reported by several researchers.

3.3.4 Analysis for adsorption equilibrium isotherms

The model for the equilibrium adsorption isotherms of Langmuir, Freundlich, Temkin, and Dubinin-Radushkevich were utilized for fitting the observed equilibrium data for the adsorption of MB dye onto the MGSAC. The parameters describing the relationship of the adsorption at equilibrium are useful in the design and development of adsorbers as well as fully understanding the adsorption processes. This relationship is used to represent how adsorbate molecules interact with the active surface sites of the adsorbent in the process. Table 2 presents the results for the comparison of constants of model expressions parameters of the adsorption isotherms with their correlation coefficients (R^2), residual sum of squares (RSS).

Table 2. Comparison of constants for model expressions of the equilibrium adsorption isotherms

Parameters	303 K	308 K	313 K	318 K
1. Model for Langmuir Adsorption Isotherms				
q_m (mg/g)	54.79	56.09	62.62	65.49
K_L (L/mg)	2.92	3.53	4.05	5.74
R^2	0.99514	0.98726	0.99285	0.99366
RSS	7.02101×10^{-6}	1.84079×10^{-5}	1.03342×10^{-5}	9.1777×10^{-6}
2. Model for Freudlich Adsorption Isotherms				
K_f $(L/mg)^{1/n}$	41.03	46.51	56.71	82.54
1/n	0.49415	0.49404	0.51032	0.57611
N	2.0237	2.0241	1.9596	1.7358
R^2	0.98156	0.94570	0.95361	0.97360
RSS	0.01311	0.03873	0.03325	0.01901
3. Model for Temkin Adsorption Isotherms				
b_T (J/mol)	192	191	189	173
A_T (L/mol)	23.75	28.92	39.20	51.31
R^2	0.97874	0.97255	0.98276	0.94116
RSS	10.65014	13.82914	8.79359	30.33749
4. Model for Dubinin-Radushkevich Adsorption Isotherms				
qe (mg/g)	45.85	47.80	51.60	56.98
β (mol^2/kJ^2)	3.6859×10^{-8}	3.1368×10^{-8}	2.60633×10^{-8}	2.09573×10^{-8}
E (kJ/mol)	5.209	5.646	6.194	6.908
R^2	0.9526	0.94843	0.98321	0.97454
RSS	0.03368	0.03679	0.01204	0.01833

3.3.5 Analysis of the models for the adsorption thermodynamics

The analysis of the models for the adsorption thermodynamics was conducted find the useful thermodynamic parameters such the changes in the standard Gibb's free energy (ΔG°), enthalpy (ΔH°), and entropy (ΔS°) in order to understand the feasibility and nature of the adsorption process. The results are presented in Table 3. The negative value of ΔG° indicates the feasibility of the adsorption process to be spontaneous. The positive values of ΔH° and ΔS° confirm that the adsorption process is endothermic and there is an increasing randomness at the interface of solid-liquid during the adsorption of MB dye adsorption onto MGSAC.

Table 3. Thermodynamic parameters of MB dye adsorption onto MGSAC

C_0 (mg/L)	ΔH (kJ/mol)	ΔS (J/mol)	ΔG (kJ/mol)				R^2	RSS
			303K	308K	313K	318K		
25	45.092	189	-12.15	0.9597	0.0119	-15.12	0.9597	0.0119
50	58.197	228	-11.13	0.9344	0.0327	-14.46	0.9344	0.0327
75	49.299	195	-9.57	0.8442	0.0595	-12.86	0.8442	0.0595
100	70.535	260	-8.73	-9.146	-10.634	-12.74	0.8718	0.0982

As temperature increases, the absolute value of ΔG^o values were also increased which indicates that high temperature is favourable for the adsorption process implying that high adsorption had been achieved at high temperatures. Positive ΔH^o values confirmed the endothermic nature of the adsorption of methylene blue onto MGSAC. The ΔH values of 45-70 kJ/mol for all initial concentrations investigated show that chemisorption may occur to enhance methylene blue adsorption. The positive value of ΔS^o which was between 189-260 J/mol for all initial concentration confirmed that there was an increase in randomness at solid/solution interface during the adsorption process (Goswami *et al*., 2017). In addition, the positive values of ΔS^o displayed by MGSAC indicated that surface changes had taken place due to the interaction of MB molecules with the surface-active sites of MGSAC (Utomo *et al*., 2015). It can be inferred that there was unequal release of energy during the adsorption process and the magnitude of $\Delta H°$ value offers information about the forces that governed the adsorption process. The enthalpy, $\Delta H°$ related to physical forces include *Vander Waals* (4–10 kJ/mol), hydrophobic interaction (5 kJ/mol), hydrogen bonding (2–40 kJ/mol), coordination exchange (40 kJ/mol), dipole bond forces (2–29 kJ/mol) and electrostatic interaction (20–80 kJ/mol) while for chemical forces (>60 kJ/mol) according to Machado *et al*., (2012).

3.3.5 Analysis for the influence of temperature and mechanism of the adsorption process

In the analysis for the influence of temperature of the MB dye adsorption and whether the mechanism of MB dye adsorption onto MGSAC is governed by physisorption or chemisorption, the modified Arrhenius-type equation for the surface coverage was employed to determine the activation energy, E_A and the sticking probability, S^*. The results of the analysis are summarized and shown in Table 4. It can be observed from results presented in Table 4 that the values of activation energy, E_A were found within the range from 44.897 to 70.213 kJ/mol for the adsorption of MB dye onto MGSAC at the initial MB dye concentrations from 25 to 100 mg/L, respectively. Positive E_A values suggest that an endothermic adsorption process, consistent with positive $\Delta H°$ values and falling within the chemisorption range. The calculated activation energy values for adsorption were all greater than 40 kJ/mol, indicating that the adsorption process was chemisorption in nature.

Table 4. Activation energy and sticking probability

C_0 (mg/L)	E_A (kJ/mol)	S*	R2	RSS
25	44.987	7.30×10^{-11}	0.96101	0.01141
50	58.084	6.39×10^{-13}	0.93117	0.03427
75	49.141	3.43×10^{-11}	0.84886	0.05716
100	70.213	1.42×10^{-14}	0.87326	0.09611

These values indicate the formation of a strong chemical interaction process between the dye molecules and the MGSAC. Generally, chemisorption generally has a high activation energy, which accounts for the high adsorption energy associated with the process. The sticking probability, S^* values were far less than unity, which indicates that the probability of the methylene blue ions to stick to surface of the modified groundnut shell activated carbon is very high. The values of sticking probability, S^* are found within the range of between 1.42×10^{-14} and 3.43×10^{-11}. These values of S^* within range of $0<S^*<1$ are considered for preferable adsorption process, and it is dependent on temperature of the system. Moreover, Najim and Yassin, (2009) have presented similar results.

4. Conclusions

Kinetics, equilibrium, and thermodynamic studies for the adsorption of MB dye adsorption onto MGSAC were successfully carried out. The research findings of this study show that activated carbon produced from groundnut shell agricultural byproducts can be successfully utilized for the adsorption of MB dye adsorption. The observed experimental data was found to be best described by pseudo 2nd order kinetic model. It was noted that the observed specific adsorption rate constant, k_{obs} decreased by 2.9 and 53 folds with increase in activation energy, E_A from 44.987 to 58.084 and to 70.213kJ/mol when the initial MB dye concentration was changed 25 mg/L to 50 mg/L and 100 mg/L, respectively. It was found that the model expression for the Langmuir equilibrium adsorption isotherm model best fitted the observed equilibrium adsorption experimental data with coefficients of determination (R^2 values) of 0.995, 0.9873, 0.9929 and 0.993 and least residual sum of square value (RSS) at operating temperature of 303 K, 308 K, 313 K, and 318 K, respectively. The maximum monolayer adsorption capacity was found to be 65.49mg/g. Thermodynamic analysis reveals that the adsorption process was endothermic and spontaneous, the changes in entropy (ΔS) were found to be between 189 and 260 J/mol while the enthalpy (ΔH) were found to be 45.092 and 70.5350 kJ/mol within the range of the initial concentration (25-100 mg/L), respectively. MGSAC was shown to be a promising adsorbent for the adsorption of MB dye from aqueous solutions with high sticking probability (S*<<1).

Acknowledgments: One of the authors Umar Isah Abubakar, PhD thanks Allah SWT for everything. The authors gratefully acknowledge the supports from Engr. Dr. Yahya Gambo for some of the analysis at King Fahd University of Petroleum and Minerals (KFUPM), Saudi Arabia, and the Department of Chemical Engineering, Ahmadu Bello University (ABU), Zaria for providing some of the research facilities.

Disclosure statements

Conflict of Interest: The authors declare that there are no conflicts of interest.

Compliance with Ethical Standards: This research article does not contain any studies involving human or animal subjects.

References

Aaddouz M., Azzaoui K., Akartasse N., Mejdoubi E., Hammouti B., Taleb M., Sabbahi R., Alshahateet S.F. (2023). Removal of Methylene Blue from aqueous solution by adsorption onto hydroxyapatite nanoparticles, *Journal of Molecular Structure*, 1288, 135807, https://doi.org/10.1016/j.molstruc.2023.135807

Abdullahi M. (2009). Production and characterization of activated carbon from carbon from Coconut shells, fruits of Flamboyant shells, and Groundnut shells, Unpublished Undergraduate Thesis, submitted to Department of Chemical Engineering, Ahmadu Bello University, Zaria.

Ahmad M. A. Puad M. A. and Bello O. S. (2014). Kinetic, equilibrium and thermodynamic studies of synthetic dye removal using pomegranate peel activated carbon prepared by microwave-induced KOH activation. *Water Resources and industry*, 6, 18-35. https://doi.org/10.1016/j.wri.2014.06.002

Al-Asadi, S. T., Al-Qaim, F. F., Al-Saedi, H. F. S., Deyab, I. F., Kamyab, H., & Chelliapan, S. (2023). Adsorption of methylene blue dye from aqueous solution using low-cost adsorbent: kinetic, isotherm adsorption, and thermodynamic studies. *Environmental Monitoring and Assessment*, *195*(6), 676. https://doi.org/10.1007/s10661-023-11334-2.

Al Othman Z.A. and Naushad M., Ali R. (2013). Kinetic, equilibrium isotherm and thermodynamic studies of Cr(VI) adsorption onto low-cost adsorbent developed from peanut shell activated with phosphoric acid. *Environmental Science Pollution Research* 20, 3351–3365. http://dx.doi.org/10.1007/s11356-012-1259-4.

Alahabadi A., Singh P., Raizada P., Anastopoulos L., Sivamani S., Dotto G. L., Landarani M., Ivanets A., Kyzas G.Z., Hosseini-Bandegharaei, A. (2020). Activated carbon from wood wastes for the removal of uranium and thorium ions through modification with mineral acid. *Colloids and Surfaces A: Physicochemical and Engineering Aspects*, 607, 125516. http://dx.doi.org/10.1016/j.colsurfa.2020.125516.

Aljeboree, A. M., Alkaim, A. F., & Al-Dujaili, A. H. (2015). Adsorption isotherm, kinetic modelling and thermodynamics of crystal violet dye on coconut husk-based activated carbon. *Desalination and Water Treatment*, *53*(13), 3656-3667. https://doi.org/10.1080/19443994.2013.877854.

Alslaibi T., Abustan I., Azmeir M. and Abu Foul A. (2013). Review: Comparison of agricultural by-products activated carbon production methods using surface area response, *International Conference on Civil Engineering (AICCE'12),* vol.2, pp.18-27.

Argun, M. E., Dursun, S., Karatas, M., & Gürü, M. (2008). Activation of pinecone using Fenton oxidation for Cd(II) and Pb(II) removal. *Bioresource Technology*, 99(18), 8691-8698. https://doi.org/10.1016/j.biortech.2008.04.014.

Arrhenius S. (1889) Über die Rektionsgeschwindigkeit bei der Inversion von Rohrzucker durch Säuren Zeitschrift für physikalische Chemie 42, 226-248. https://doi.org/10.1515/zpch-1889-0416

Augustine E. Ofomaja; Yuh-Shan Ho (2007). Effect of pH on cadmium biosorption by coconut copra meal. , 139(2), 356–362. doi:10.1016/j.jhazmat.2006.06.039.

Bello, O. S., and Ahmad, M. A. (2012). Coconut (*Cocos nucifera*) shell based activated carbon for the removal of malachite green dye from aqueous solutions. *Separation Science and Technology*, 47(6), 903-912. https://doi.org/10.1080/01496395.2011.630335.

Danish, M., Ahmad, T., Majeed, S., Ahmad, M., Ziyang, L., Pin, Z., & Iqubal, S. S. (2018). Use of banana trunk waste as activated carbon in scavenging methylene blue dye: Kinetic, thermodynamic, and isotherm studies. *Bioresource Technology Reports*, *3*, 127-137. https://doi.org/10.1016/j.biteb.2018.07.007

Darré, L., Machado, M. R., Brandner, A. F., González, H. C., Ferreira, S., & Pantano, S. (2015). SIRAH: a structurally unbiased coarse-grained force field for proteins with aqueous solvation and long-range electrostatics. *Journal of chemical theory and computation*, 11(2), 723-739. https://doi.org/10.1021/ct5007746.

Das, A.; Mishra, S. (2017). Removal of textile dye reactive green-19 using bacterial consortium: Process optimization using response surface methodology and kinetics study. Journal of Environmental Chemical Engineering, 5(1), 612–627. http://dx.doi.org/10.1016/j.jece.2016.10.005.

Dubinin, M. (1960). The potential theory of adsorption of gases and vapors for adsorbents with energetically nonuniform surfaces. *Chemical reviews*, 60(2), 235-241. https://doi.org/10.1021/cr60204a006.

Ebrahimi, A. Pajootan, E. Arami, M., Bahrami, M. (2013) Optimization, kinetics, equilibrium, and thermodynamic investigation of cationic dye adsorption on the fish bone. *Desalin Water Treat* 53, 1-11. http://dx.doi.org/10.1080/19443994.2013.860631

Elg, A. P., Eisert, F., Rosén, A. (1997). The temperature dependence of the initial sticking probability of oxygen on Pt (111) probed with second harmonic generation. *Surface science*, 382(1-3), 57-66. https://doi.org/10.1016/S0039-6028(97)00096-4

Foo, K. Y., and Hameed, B. H. (2010). An overview of dye removal via activated carbon adsorption process. *Desalination and Water Treatment*, 19(1-3), 255-274. https://doi.org/10.5004/dwt.2010.1214.

Freundlich H. (1907) Ueber Kolloidfällung und Adsorption. Zeitschrift für Chemie und Industrie der Kolloide. 1**,** 321-331. https://doi.org/10.1007/BF01813604.

Fu, Jianwei, Zhonghui Chen, Minghuan Wang, Shujun Liu, Jinghui Zhang, Jianan Zhang, Runping Han, and Qun Xu (2015). "Adsorption of methylene blue by a high-efficiency adsorbent (polydopamine microspheres): kinetics, isotherm, thermodynamics and mechanism analysis." *Chemical Engineering Journal* 259: 53-61. https://doi.org/10.1016/j.cej.2014.07.101.

Hameed, B. H. Ahmad, A. A. Aziz, N. (2007) Isotherms, kinetics, and thermodynamics of acid dye adsorption on activated palm ash. *Chem. Eng. J.* 133, 195-203. https://doi.org/10.1016/j.cej.2007.01.032

Ho, Y. S.; McKay, G. (1999) Pseudo-Second Order Model for Sorption Processes. *Process Biochem.*, 34 620 (5), 451–465. https://doi.org/10.1016/S0032-9592(98)00112-5

Isah U. A, Ibrahim A., Giwa A., Muhammad S., Abdullahi M. (2022) Kinetics, equilibrium and thermodynamics studies of Direct Red 1 dye adsorption on groundnut shell based activated carbon. *J. Mater. Environ. Sci.*, 2022, 13(9), 988-1002. http://www.jmaterenvironsci.com.

Isah U. A,, Abdullahi A, and Hamza A. (2023). Adsorption of Methylene Blue Dye onto modified activated carbon produced from groundnut shells. *J. Mater. Environ. Sci*. 14 (8) 947-966. http://www.jmaterenvironsci.com.

Isah U. A,, Giwa A., Bala S., Muhammad S., Abdullahi M. (2015). Kinetics, equilibrium, and thermodynamics studies of C.I. Reactive Blue 19 Dye adsorption on Coconut shell based activated carbon. Inter. *Biodeterioration & Biodegradation Journal.* 102, 265-273. https://doi.org/10.1016/j.ibiod.2015.04.006.

Islam, M. A., Tan, I. A. W., Benhouria, A., Asif, M., & Hameed, B. H. (2015). Mesoporous and adsorptive properties of palm date seed activated carbon prepared via sequential hydrothermal carbonization and sodium hydroxide activation. *Chemical Engineering Journal*, *270*, 187-195. https://doi.org/10.1016/j.cej.2015.01.058.

Jawad, A. H., Hum, N. N. M. F., Farhan, A. M., and Mastuli, M. S. (2020). Biosorption of methylene blue dye by rice (Oryza sativa L.) straw: adsorption and mechanism study. *Desalin Water Treat*, *190*, 322-330. https://doi.org/10.5004/dwt.2020.25644.

Kalavathy M.H., Regupathi I., Pillai M.G., Miranda L.R. (2009). Modeling, analysis and optimization of adsorption parameters for H_3PO_4 activated rubber wood sawdust using response surface methodology (RSM). *Colloids Surf B* 70, 35–45. https://doi.org/10.1016/j.colsurfb.2008.12.007.

Kankou M. S.'A., N'diaye A. D., Hammouti B., Kaya S. and Fekhaoui M. (2021) Ultrasound-assisted adsorption of Methyl Parathion using commercial Granular Activated Carbon from aqueous solution, *Mor. J. Chem.* 9(4), 832-842

Kumari, G., Soni, B., Karmee, S. K. (2020). Synthesis of Activated Carbon from Groundnut Shell Via Chemical Activation. *Journal of The Institution of Engineers, India* https://doi.org/10.1007/s40034-020-00176-z.

Lagergren S. (1898) Zur theorie der sogenannten adsorption gelöster stoffe. Kungliga Svenska Vetenskapsakademiens. Handlingar, Band 24:1-39. https://sid.ir/paper/572485/en

Langmuir I. (1916) The constitution and fundamental properties of solids and liquids. Part I Solids, *J of the Ame. Chem. Soc.* 38:2221-2295. https://doi.org/10.1021/ja02268a002

Li, H. An, N. Liu, G. Li, J., Liu, N., Jia, M., Zhang, W. Yuan, X. (2015). Adsorption behaviors of methyl orange dye on nitrogen-doped mesoporous carbon materials. *Journal of Colloid and Interface Science*, S002197971530432X. https://doi.org/10.1016/j.jcis.2015.12.048

Li, L. Quinlivan P.A. Knappe D.R.U., (2002). Effects of activated carbon surface chemistry and pore structure on the adsorption of organic contaminants from aqueous solution. *Carbon* 40 (12), 2085–2100. https://doi.org/10.1016/S0008-6223(02)00069-6.

Lin, D., Wu, F., Hu, Y., Zhang, T., Liu, C., Hu, Q. HKo, T. (2020). Adsorption of dye by waste black tea powder: parameters, kinetic, equilibrium, and thermodynamic studies. *Journal of Chemistry*, 2020.

Muhammad S. (2010). Optimization of the production of activated carbon produced from from Groundnut shells, Unpublished Undergraduate Thesis, submitted to Department of Chemical Engineering, Ahmadu Bello University, ZarMohammed

Najim T.S., Yassin S.A. (2009). Removal of chromium from aqueous solution using modified pomegranate peel: mechanistic and thermodynamic studies. *Journal of Chemistry*, *6*, S153-S158. doi.org/10.1155/2009/804256

Oladipo M.A., Bello I.A., Adeoye D.O., Abdulsalam, K.A., Giwa, A.A. (2013). Sorptive Removal of Dyes from Aqueous Solution: A Review. *Advances in Environmental Biology*, 7(11), 3311-3327.

Oladoye P.O., Ajiboye T.O., Omotola E.O., Oyewola O.J. (2022), Methylene blue dye: Toxicity and potential elimination technology from wastewater, *Results in Engineering*, 16, 100678, ISSN 2590-1230, https://doi.org/10.1016/j.rineng.2022.100678

Qiu, M., Xuan, Y., Luo, P., Wang, Z., & Shou, J. (2015). Adsorption of methylene blue by activated carbon from capsicum straw. *Nature Environment and Pollution Technology*, *14*(4), 859. ISSN: 0972-6268.

Rafatullah M., Sulaiman O., Hashim R., Ahmad A. (2010). Adsorption on methyhlene blue on low cost adsorbent: A review. *J. Hazard. Meter,* 177, 1, pp.70–80. https://doi.org/10.1016/j.jhazmat.2009.12.047.

Rasool, K., and Lee D. S. (2015) Characteristics, kinetics, and thermodynamics of Congo Red biosorption by activated sulfidogenic sludge from an aqueous solution. *Int. J. Environ. Sci. Technol.* 12(2), 571-580.

Saka, C. (2012). BET, TG-DTG, FT-IR, SEM, Iodine Number Analysis and Preparation of Activated Carbon from Acorn Shell by Chemical Activation with ZnCl2. *J. Analytical and Applied Pyrolysis*, 95, 21-24. https://doi.org/10.1016/j.jaap.2011.12.020.

Salman J.M. and Alsaad K. (2012). Adsorption of 2,4-dichlorophenoxyacetic acid onto date seeds activated carbon: Equilibrium, Kinetic and thermodynamic studies‖ *Int. J. Chem. Sci.*, 10, no.2, 677-690. . https://www.researchgate.net/publication/258129204

Sarabadan, M., Bashiri, H., Mousavi, S. M. (2019). Removal of crystal violet dye by an efficient and low-cost adsorbent: Modeling, kinetic, equilibrium and thermodynamic studies. *Korean Journal of Chemical Engineering*, 36(10), 1575-1586. https://doi.org/10.1007/s11814-019-0356-1

Sekirifa M.L., Hadj-Mohamed M., Pallier S., Baameur L., Richard D., Al-Dujaili A.H. (2013). Preparation and characterization of an activated carbon from a date stones variety by physical activation with carbon dioxid, *Journal of Analytical and Applied Pyrolysis*, 99(1), 155–160. http://dx.doi.org/10.1016/j.jaap.2012.10.007.

Shi, Li; Zhang, Ge; Wei, Dong; Yan, Tao; Xue, Xiaodong; Shi, Shusheng; Wei, Qin (2014). Preparation and utilization of anaerobic granular sludge-based biochar for the adsorption of methylene blue from aqueous solutions. *Journal of Molecular Liquids*, 198, 334–340. doi:10.1016/j.molliq.2014.07.023

Shitu, M.A., Ibrahim A. (2014). Removal of Methylene Blue Using Low Cost Adsorbent: A Review Research, *Journal of Chemical Sciences*, 4(1), 91-102. https://www.researchgate.net/publication/267737463

Sivashankar R., Sathya A.B., Vasantharaj K., Sivasubramanian V. (2014) Magnetic composite an environmental super adsorbent for dye sequestration – a review, *Environ. Nanotechnol. Monit. Manag.*, 1–2, pp. 36-49

Sulaiman, N.S., Mohamad Amini, M.H., Danish, M., Sulaiman, O., Hashim, R. (2021). Kinetics, Thermodynamics, and Isotherms of Methylene Blue Adsorption Study onto Cassava Stem Activated Carbon. *Water*, 13, 2936. https://doi.org/10.3390/w13202936

Temkin, M. I. (1940). Kinetics of ammonia synthesis on promoted iron catalysts. *Acta Phys. Chim. USSR*, 12, 327-356.

Teshome, A. (2015). Preparation, Characterization and Application of Coffee Husk Based Activated Carbon for Adsorption of Cr(VI) from Aqueous Solution. School of Chemical and Bio Engineering, Addis Ababa Institute of Technology, Addis Ababa University.

Timur S., Kantarli I. C., Ikizoglu E., Yanik J. (2006). Preparation of activated carbons from Oreganum stalks by chemical activation. *Energy and Fuels*, 20(6), 2636–2641. https://doi.org/10.1021/EF060219K.

Torğut, G., Demirelli, K. (2018). Comparative adsorption of different dyes from aqueous solutions onto polymer prepared by ROP: kinetic, equilibrium and thermodynamic studies. *Arabian Journal for Science and Engineering*, 43(7), 3503-3514. https://doi.org/10.1007/s13369-017-2947-7.

Vernersson T., Bonelli P. R., Cerrella E. G. and Cukierman A. L. (2002). Arundo donax cane as a precursor for activated carbons preparation by phosphoric acid activation. *Bioresource Technology*, 83, no. 2, 95–104. https://doi.org/10.1016/S0960-8524(01)00205-X.

Wang, J., Wang, Y., Liu, H., Zhang, J. Zhang, C. Wang, J. (2016). Sorption of Ni(II) by Fe(II) and EDTA-modified activated carbon derived from pyrophosphoric acid activation, Desalination Water Treatment 57 3700–3707. http://dx.doi.org/10.1080/19443994.2014.989917

Wang, Shuang; Nam, Hoseok; Nam, Hyungseok (2020). Preparation of activated carbon from peanut shell with KOH activation and its application in H2S adsorption: isotherm and kinetic studies. J. Environ. Chemical Engineering, http://dx.doi.org/10.1016/j.jece.2020.103683.

Weber, W., Morris J. (1963) Kinetics of adsorption on carbon from solution. J. Sanit Eng. Div. Am. Soc. Civ. Eng. 89:31-60. https://doi.org/10.1061/JSEDAI.0000430.

Wu H., Chen R., Du H. (2019) Synthesis of activated carbon from peanut shell as dye adsorbents for wastewater treatment. *Adsorption Science & Technology*, 37(1-2), 34-48. http://dx.doi.org/10.1177/0263617418807856.

Yaqub M, Sen T, Afroze S., Ang, H, (2014). Dye and its removal from aqueous solution by adsorption: a review. *Adv. Colloid Interface Sci.* 20 (9), 172–184. http://dx.doi.org/10.1016/j.cis.2014.04.002

Yaseen, D, Scholz, M, (2018). Treatment of synthetic textile wastewater containing dye mixtures with microcosms. *Environ. Sci. Pollut. Control Ser.* 25 (2),1980–1997. https://doi.org/10.1007/s11356-017-0633-7.

Zoha Heidarinejad, Mohammad Hadi Dehghani, Mohsen Heidari, Gholamali Javedan, Imran Ali, Mika Sillanpää (2020). Methods for preparation and activation of activated carbon: a review. *Environmental Chemistry Letters*. Vol.:(0123456789, Springer Nature Switzerland AG 2020. https://doi.org/10.1007/s10311-019-00955-0.

Zubair, M., Jarrah, N. M., Manzar, S. Al-Harthi, M., Daud, M., Mu'azu, N. D., Haladu, N. D. (2017). Adsorption of eriochrome black T from aqueous phase on MgAl-, CoAl-and NiFe-calcined layered double hydroxides: kinetic, equilibrium and thermodynamic studies. *Journal of molecular liquids*, *230*, 344-352. https://doi.org/10.1016/j.molliq.2017.01.031.